Comparative modeling studies of lanosterol 14-α demethylase of *Moniliophthora perniciosa*

Estudos de Modelagem Comparativa da lanosterol 14-α demetilase de *Moniliophthora perniciosa*

Títulos abreviados:

Modeling of lanosterol 14-α demethylase of M. perniciosa

Modelagem da lanosterol 14-α demetilase de M. perniciosa

Alessandra Gomes Marques Pacheco[1], Marcelo Santos Castilho[1,2], Angélica Maria Lucchese[1], Gonçalo Pereira[3], Alex Gutterres Taranto*[4]

ABSTRACT

Moniliophthora perniciosa is the causative agent of witches' broom, which affects the *Theobroma cacao*, causing great losses in cocoa production. The integrated management techniques available allow controlling the pest only partially. An important strategy to contain the witches' broom is to study the interactions of the enzyme lanosterol 14α-demethylase (CYP51) of *Moniliophthora* with azole compounds. These compounds block the synthesis of ergosterol and consequently the fungal growth by the connection between the iron atom in the cofactor of this enzyme and the nitrogen atom of the azole. However, there is no study on the interaction of these compounds with the enzyme lanosterol 14α-demethylase of this pathogen. In this work, a model of the enzyme lanosterol 14α-demethylase of *M. perniciosa* was created by comparative modeling techniques. Then, the spatial arrangement of residues that comprise the catalytic site of the enzyme was identified. The results obtained are in agreement with the crystallographic CYP51. The results show that the built model can be used for molecular modeling and *de novo* design studies.

Keywords: *Moniliophthora perniciosa*, molecular modeling, azole compounds, CYP51.

RESUMO

Moniliophthora perniciosa é o agente causador da vassoura de bruxa, que afeta o *Theobroma cacao*, causando grandes perdas na produção de cacau. As técnicas de gestão integrada desenvolvidas permitem controlar a praga apenas parcialmente. Uma estratégia importante para conter a vassoura de bruxa é estudar as interações da enzima lanosterol 14α-demethylase (CYP51) de *Moniliophthora* com compostos azólicos. Estes compostos bloqueiam a síntese de ergosterol e, consequentemente, o crescimento fúngico pela ligação entre o átomo de ferro do cofactor dessa enzima e o átomo de nitrogênio do grupo azol. No entanto, não há um estudo sistemático sobre a interação destes compostos com a enzima lanosterol 14α-demetilase deste patógeno. Neste trabalho, um modelo da enzima lanosterol 14α-demetilase do *M. perniciosa* foi criado por técnicas de modelagem comparativa. Em seguida, o arranjo espacial dos resíduos que formam o sítio catalítico da enzima foi identificado. Os resultados mostram que o modelo construído pode ser empregado em estudos de ancoragem molecular e *de novo* design.

Palavras-chave: *Moniliophthora perniciosa*, modelagem molecular, compostos azóis, CYP51.

[1] Programa de Pós-graduação em Biotecnologia (PPGBiotec UEFS/CPqGM/FIOCRUZ), Universidade Estadual de Feira de Santana, Feira de Santana, Bahia, Brasil.
[2] Laboratório de Bioinformática, Faculdade de Farmácia, Universidade Federal da Bahia, Salvador, Brasil.
[3] Biology Institute, State University of Campinas (UNICAMP), Zeferino Vaz, University City, 6109, Campinas, SP-Brazil, 23083-970
[4*] Programas de Pós-Graduação em Biotecnologia e Ciências Farmacêuticas, Laboratório de Modelagem Molecular, Campus Centro-Oeste (CCO), Universidade Federal de São João del-Rei, Divinópolis, Minas Gerais, Brasil. Autor para correspondência: proftaranto@hotmail.com

INTRODUCTION

The basidiomycete *Moniliophthora perniciosa* (AIME; PHILLIPS-MORA, 2005) is a hemibiotrophic fungus that causes the witches' broom disease, which has become of the spreading phytopathological problem of the producing regions of *Theobroma cacao* in the American continent (THOMAZELLA *et al.*, 2012; ZAPAROLI *et al.*, 2009).
In Brazil, this pathogen was identified in 1989 in the south of Bahia State, a region of cocoa intensive plantation, causing an impact on the local economy. In consequence of the spread of witches' broom, Brazil, which ranked second in world exports, began importing the fruit. The reflection on the local economy was immediate, because the eradication of producing areas led to unemployment of many rural workers (THOMAZELLA et al., 2012; ZAPAROLI et al., 2009).

According to previous work, several efforts have been performed for the disease control. However, the forms of control so far have low efficiency (THOMAZELLA et al., 2012; ZAPAROLI et al., 2009). Currently, several efforts have been made in the elucidation of molecular targets (JUNIOR *et al.*, 2013; PINHEIRO *et al.*, 2012; SANTOS *et al.*, 2011; SENA *et al.*, 2011). An alternative to combating the witches' broom is the use of inhibitors of sterol biosynthesis (SBIs). The SBIs include structurally diverse chemical compounds, including azole compounds, which target the lanosterol 14α-demethylase (CYP51 of *M. perniciosa*), which catalyzes redox reactions, acting in the biosynthesis of sterols. Overall, the CYP51 are formed by α-helices and β-sheets surrounding the heme (prosthetic group) of the enzyme. The active site consists of a hydrophobic domain for substrate binding, which is the prosthetic group with an iron atom bound to four pyrrole rings (ALCAZAR-FUOLI *et al.*, 2008).

The CPY51 found in fungi have been identified as integral membrane proteins, which makes the biophysical characterization extremely complex. The elucidation of the structure of CYP51 from *Mycobacterium tuberculosis* (MT-CYP51) has facilitated the study of different fungi CPY51s (OUELLET *et al.*, 2010). In this context, the enzyme CPY51 *M. perniciosa* (MP-CPY51) has not had their 3D structure elucidated yet. Our studies aimed to generate a 3D model by comparative modeling using structures of MT-CYP51. These results will be used for docking studies between model and azole inhibitors, showing the principal interactions involved between MP-CYP51 and azoles (OUELLET *et al.*, 2011). These studies can suggest a pharmacophoric model to develop new active compounds more selective and effective against witches' broom.
The release of MP-CPY51, which has 555 amino acids, motivates us to build a model (WOO *et al.*, 2002). Next, BLASTp (ALTSCHUL *et al.*, 1990) server was used to identify sequences homologous to MP-CPY51. The alignment of amino acid sequence of MP-CPY51 with its templates was performed with the program CLUSTAL W (LARKIN *et al.*, 2007).

MATERIAL AND METHODS

The model MP-CPY51 was built using program SWISS-MODEL, following a previously established protocol (BORDOLI *et al.*, 2009; LEMUCHI *et al.*, 2013). The residues composing the active site were identified within a radius of 4.5 Å determined by the selection of inhibitor present in the template obtained in the previous step. After generating the model, the atomic coordinates of the heme was transferred from the template to the model. The model was optimized in the AMBER 9.0 program (PEARLMAN *et al.*, 1995). The model was prepared by LEaP, and refined by SANDER using the FF03 force field (DUAN *et al.*, 2003). In addition, heme parameters were prepared using the semi-empirical method PM6 (FREITAS *et al.*, 2012;

STEWART, 2007). A full optimization was carried out by steepest descent and conjugate gradient algorithms in Generalized Born implicit solvent (STILL *et al.*, 1990). Finally, the model was evaluated by PROCHECK, ANOLEA and VERIFY 3D software (EISENBERG; LUTHY; BOWIE, 1997; LASKOWSKI *et al.*, 1993; MELO; FEYTMANS, 1998).

RESULTS AND DISCUSSION

Three crystal structures were used to construct the model MP-CPY51 with 30% of identity. These were deposited in the Protein Data Bank with codes 1E9X, 2VKU and 2W0B (CHEN *et al.*, 2009; EDDINE *et al.*, 2008; PODUST; POULOS; WATERMAN, 2001), which are complexed with their respective inhibitors. As these three templates have different inhibitors; their structures could contribute to the construction of the more robust model to the MP-CYP51. As can be seen in Figure 1, the α-helix involved in the membrane insertion, located in the N-terminal sequence of MP-CYP51, is not present in the templates structures and their amino acids are not part of the active site. Thus, this area was neglected during the construction of the model.

Figure 1 Multiple alignment performed by Clustal W on amino acid sequence of the 14αDM of the *M. perniciosa* and amino acid sequences corresponding to structures with PDB codes 2W0B, and 2VKU 1E9X. Regions highlighted in green, red region and the active site cysteine that binds to the heme group, respectively.

The resulting model had 22 α-helices, 16 β-sheets, 16 loops and similar structural characteristics with other CYP51s (Figure 2a). Additionally, the heme is complexed with the ilcarbamate inhibitor within the enzyme, confirming the hydrophobic character of parts of the active site of the enzyme, which were located within 4.5 Å from inhibitor. The active site was identified as His76, Leu77, Met96, Gln98, Lys99, Lys100, Phe101, Ala 261, 265 Ala Met264, His268, Thr269, Ile334, Cys407, and Tyr447. The overlap of the CYP51 model MP-1E9X, and 2VKU 2W0B using the Cα as reference (Figure 2) shows the root-mean-square deviation (RMSD) of 2.22 Å and 2.38 Å and 2.47 Å, respectively. This high value of RMSD is due to low similarity between sequences and very flexible regions.

Figure 2 a) 3D MP-CYP51 structure built by comparative modeling. Highlighted in pink and blue are the heme group and inhibitor 3-{(4-methylphenyl) sulfonyl amino-4-propylpyridine ilcarbamate, respectively}, b) structural alignment with Cαs between MP-CYP51 (red), 1E9X (blue), 2VKU (yellow) and 2W0B (green).

A)   **B)**
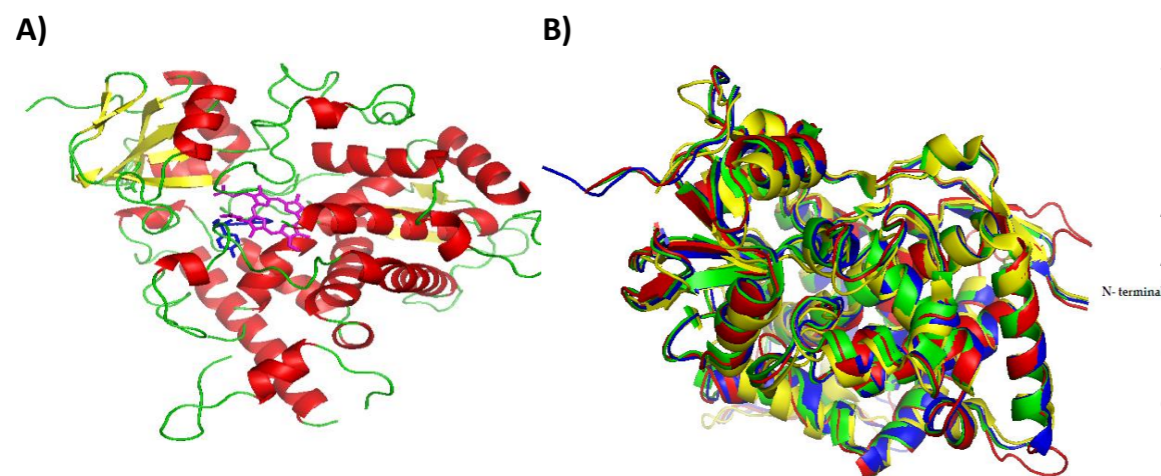
The constructed model was refined with implicit solvent model using AMBER9 software, and evaluated by three different methodologies (ANOLEA, PROCHECK, and VERIFY 3D). The ANOLEA program calculates the

sum of interaction of atoms within a radius of 7 Å for each amino acid resulting in the potential energy profile of the structure of a protein, which demonstrates how the chemical environment around the atom contributes to its stability. Figure 3 shows the graph of potential energy for each amino acid obtained by ANOLEA. The potential energy is -1.641/kT, where 14% amino acid residues have positive values after the optimization of energy. However, these residues were not observed in the active site residues. The PROCHECK program evaluates the accuracy of the overall structure and stereochemistry of each residue individually. Figure 4 shows the validation obtained by PROCHECK. As can be seen, 98.1% of the amino acids are in energetically favorable regions (favorable and allowed regions), and the region acceptable is found 1.4% of amino acids found in acceptable region and only 0.5% are in the unfavorable region and correspond to residues Gln136, Pro348, Pro349, Ala403. These resides are not present in the active site model and are located in the loops that are flexible regions in the protein. Finally, the VERIFY 3D program measures the compatibility between the sequence of amino acid of the protein and the model of its 3D structure The graphics of VERIFY (Figure 5) shows regions that are below 0, indicating incompatibility problems between sequence and structure. However, after identifying the residues lying in that region (Val87, Tyr88, Asn92, Val94, Phe95, Met96, Gln295, Val296, Lys297, His298, Pro349, Ala353, Glu356), it was observed that it is not constitute the active site of model as well. The validations have demonstrated that the model MP-CYP51 has low potential energy, excellent stereochemistry quality with high compatibility with the targets structure.
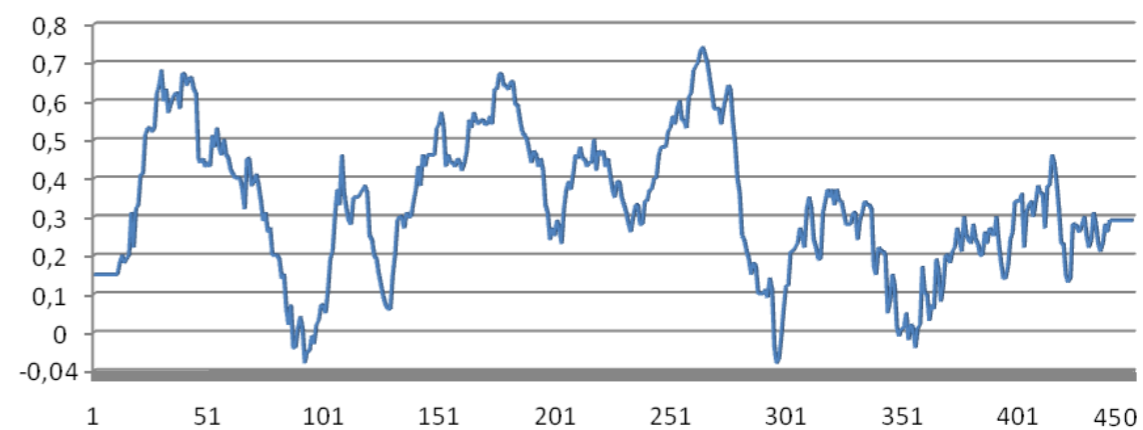
Figure 3 Graphic of ANOLEA (potential energy of each atom in the protein chain). After optimization of the model with the total energy (641/kT).
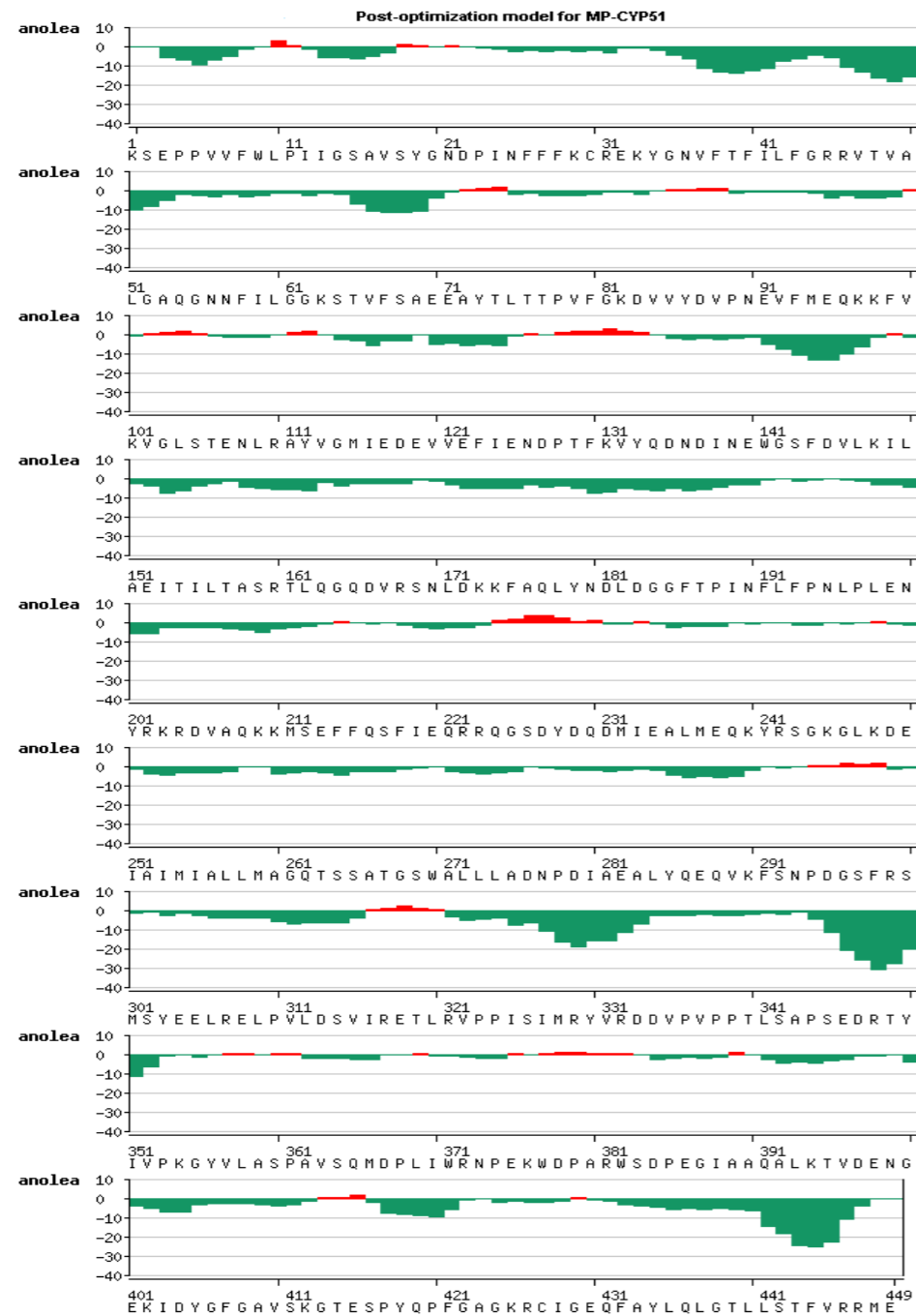
Figure 4 Validation obtained through PROCHECK program. Ramachandran plot of MP-CYP51 model shows that 98.1% of the amino acids are in energetically favorable regions.
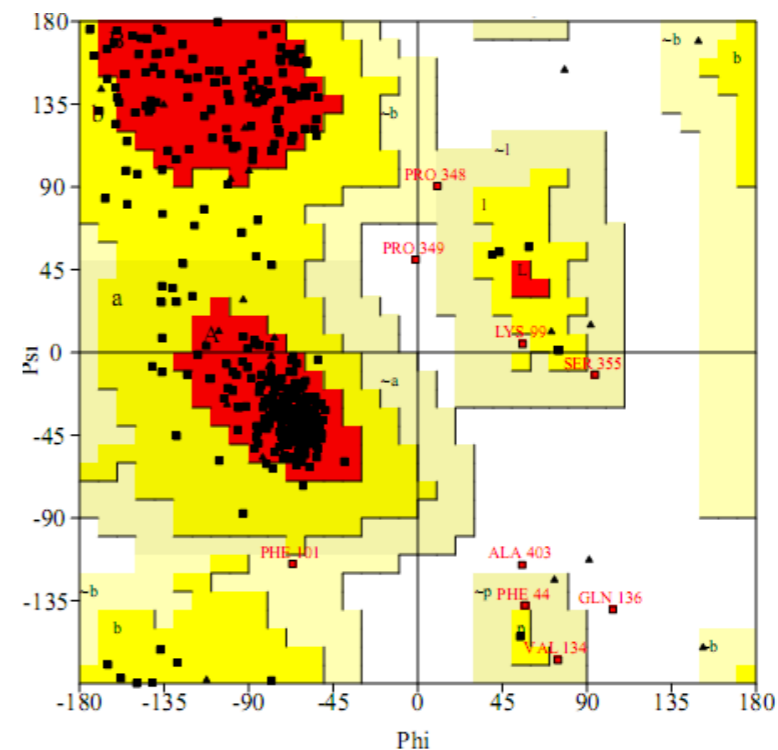
Figure 5 Verify 3D Graphic of the MP-CYP51 model

In this work, the three dimensional structure of the CPY51 of *M. perniciosa* (MP-CPY51), previously unknown, was built by comparative modeling techniques based on crystal structures 1E9X, 2VKU and 2W0B, and refined by molecular mechanics. The MP-CPY51 structure was validated by ANOLEA, PROCHECK and VERIFY 3D. Following comparative modeling studies, azole inhibitors such as difenoconazole, miconazole, prothioconazol, sulconazol will be docked against this model in order to study the intermolecular interaction. These data can permit to build a pharmacophore model for identification of a minimum structural requirement for activity. Thus, this study provided an initial step for construction and identification of new inhibitors against MP-CPY51.

ACKNOWLEDGEMENTS

REFERENCES

AIME, M. C.; PHILLIPS-MORA, W. The causal agents of witches' broom and frosty pod rot of cacao (chocolate, Theobroma cacao) form a new lineage of Marasmiaceae. **Mycologia,** v. 97, n. 5, p. 1012-1022, 2005.

ALCAZAR-FUOLI, L.; MELLADO, E.; GARCIA-EFFRON, G.; LOPEZ, J. R.; GRIMALT, J. O.; CUENCA-ESTRELLA, J. M.; RODRIGUEZ-TUDELA, J. L. Ergosterol biosynthesis pathway in Aspergillus fumigatus. **Steroids,** v. 73, n. 3, p. 339-347, 2008.

ALTSCHUL, S. F.; GISH, W.; MILLER, W.; MYERS, E. W.; LIPMAN, D. J. Basic Local Alignment Search Tool. **Journal of Molecular Biology,** v. 215, n. 3, p. 403-410, 1990.

BORDOLI, L.; KIEFER, F.; ARNOLD, K.; BENKERT, P.; BATTEY, J.; SCHWEDE, T. Protein structure homology modeling using SWISS-MODEL workspace. **Nature Protocols,** v. 4, n. 1, p. 1-13, 2009.

CHEN, C. K.; DOYLE, P. S.; YERMALITSKAYA, L. V.; MACKEY, Z. B.; ANG, K. K. H.; MCKERROW, J. H.; PODUST, L. M. Trypanosoma cruzi CYP51 Inhibitor Derived from a Mycobacterium tuberculosis Screen Hit. **Plos Neglected Tropical Diseases,** v. 3, n. 2, 2009.

DUAN, Y.; WU, C.; CHOWDHURY, S.; LEE, M. C.; XIONG, G. M.; ZHANG, W.; YANG, R.; CIEPLAK, P.; LUO, R.; LEE, T.; CALDWELL, J.; WANG, J. M.; KOLLMAN, P. A point-charge force field for molecular mechanics simulations of proteins based on condensed-phase quantum mechanical calculations. **Journal of Computational Chemistry,** v. 24, n. 16, p. 1999-2012, 2003.

EDDINE, A. N.; VON KRIES, J. P.; PODUST, M. V.; WARRIER, T.; KAUFMANN, S. H. E.; PODUST, L. M. X-ray structure of 4,4 '-dihydroxybenzophenone mimicking sterol substrate in the active site of sterol 14 alpha-demethylase (CYP51). **Journal of Biological Chemistry,** v. 283, n. 22, p. 15152-15159, 2008.

EISENBERG, D.; LUTHY, R.; BOWIE, J. U. VERIFY3D: Assessment of protein models with three-dimensional profiles. **Macromolecular Crystallography, Pt B,** v. 277, p. 396-404, 1997.

FREITAS, J. A. D.; GARIB, D. G.; OLIVEIRA, T. M.; LAURIS, R. D. M. C.; DE ALMEIDA, A. L. P. F.; NEVES, L. T.; TRINDADE-SUEDAM, I. K.; YAEDU, R. Y. F.; SOARES, S.; PINTO, J. H. N. Rehabilitative treatment of cleft lip and palate: experience of the Hospital for Rehabilitation of Craniofacial Anomalies - USP (HRAC-USP) - Part 2: Pediatric Dentistry and Orthodontics. **Journal of Applied Oral Science,** v. 20, n. 2, p. 268-281, 2012.

JUNIOR, M. C.; DE ASSIS, S. A.; GOES-NETO, A.; DUARTE, A. A.; ALVES, R. J.; TARANTO, A. G. Structure-based drug design studies of UDP-N-acetylglucosamine pyrophosphosrylase, a key enzyme for the control of witches' broom disease. **Chem Cent J,** v. 7, n. 1, p. 48, 2013.

LARKIN, M. A.; BLACKSHIELDS, G.; BROWN, N. P.; CHENNA, R.; MCGETTIGAN, P. A.; MCWILLIAM, H.; VALENTIN, F.; WALLACE, I. M.; WILM, A.; LOPEZ, R.; THOMPSON, J. D.; GIBSON, T. J.; HIGGINS, D. G. Clustal W and clustal X version 2.0. **Bioinformatics,** v. 23, n. 21, p. 2947-2948, 2007.

LASKOWSKI, R. A.; MACARTHUR, M. W.; MOSS, D. S.; THORNTON, J. M. Procheck - a Program to Check the Stereochemical Quality of Protein Structures. **Journal of Applied Crystallography,** v. 26, p. 283-291, 1993.

LEMUCHI, M. O.; VIEIRA, M. S.; GRANJEIRO, P. A.; DA SILVA, J. A.; LIMA, W. J. N.; GONÇALVES, D. B.; GALDINO, A. S.; COMAR JR, M.; TARANTO, A. G. Uso de modelagem comparativa na determinação estrutural de fitase de Yersinia. **BBR - Biochemistry and Biotechnology Reports,** v. 2, n. 1, p. 25-30, 2013.

MELO, F.; FEYTMANS, E. Assessing protein structures with a non-local atomic interaction energy. **Journal of Molecular Biology,** v. 277, n. 5, p. 1141-1152, 1998.

OUELLET, H.; GUAN, S. H.; JOHNSTON, J. B.; CHOW, E. D.; KELLS, P. M.; BURLINGAME, A. L.; COX, J. S.; PODUST, L. M.; DE MONTELLANO, P. R. O. Mycobacterium tuberculosis CYP125A1, a steroid C27 monooxygenase that detoxifies intracellularly generated cholest-4-en-3-one. **Molecular Microbiology,** v. 77, n. 3, p. 730-742, 2010.

OUELLET, H.; KELLS, P. M.; DE MONTELLANO, P. R. O.; PODUST, L. M. Reverse type I inhibitor of Mycobacterium tuberculosis CYP125A1. **Bioorganic & Medicinal Chemistry Letters,** v. 21, n. 1, p. 332-337, 2011.

PEARLMAN, D. A.; CASE, D. A.; CALDWELL, J. W.; ROSS, W. S.; CHEATHAM, T. E.; DEBOLT, S.; FERGUSON, D.; SEIBEL, G.; KOLLMAN, P. Amber, a Package of Computer-Programs for Applying Molecular Mechanics, Normal-Mode Analysis, Molecular-Dynamics and Free-Energy Calculations to Simulate the Structural and Energetic Properties of Molecules. **Computer Physics Communications,** v. 91, n. 1-3, p. 1-41, 1995.

PINHEIRO, A. A. F.; TARANTO, A. G.; DUARTE, A. A.; NETO, A. G.; DA HORA, B. T.; PEREIRA, G. A. G.; DOS SANTOS, M. C.; DE ASSIS, S. A. Homology modeling studies of beta(1,3)-D-glucan synthase of Moniliophthora perniciosa. **International Journal of Quantum Chemistry,** v. 112, n. 20, p. 3356-3363, 2012.

PODUST, L. M.; POULOS, T. L.; WATERMAN, M. R. Crystal structure of cytochrome P450 14 alpha-sterol demethylase (CYP51) from Mycobacterium tuberculosis in complex with azole inhibitors. **Proceedings of the National Academy of Sciences of the United States of America,** v. 98, n. 6, p. 3068-3073, 2001.

SANTOS, M. C.; GONCALVES, P. A.; TARANTO, A. G.; KOBLITZ, M. G. B.; GOES-NETO, A.; PIROVANI, C. P.; CASCARDO, J. C. M.; DA CRUZ, S. H.; ZINGALI, R. B.; PEREIRA, G. A. G.; DIAS, C. V.; DE ASSIS, S. A. Purification, Characterization and Structural Determination of UDP-N-Acetylglucosamine Pyrophosphorylase Produced by Moniliophthora perniciosa. **Journal of the Brazilian Chemical Society,** v. 22, n. 6, p. 1015-U264, 2011.

SENA, A. R.; JUNIOR, G. L. V.; NETO, A. G.; TARANTO, A. G.; PIROVANI, C. P.; CASCARDO, J. C. M.; ZINGALI, R. B.; BEZERRA, M. A.; ASSIS, S. A. Production, purification and characterization of a thermostable beta-1,3-glucanase (laminarinase) produced by Moniliophthora perniciosa. **Anais Da Academia Brasileira De Ciencias,** v. 83, n. 2, p. 599-609, 2011.

STEWART, J. J. P. Optimization of parameters for semiempirical methods V: Modification of NDDO approximations and application to 70 elements. **Journal of Molecular Modeling,** v. 13, n. 12, p. 1173-1213, 2007.

STILL, W. C.; TEMPCZYK, A.; HAWLEY, R. C.; HENDRICKSON, T. Semianalytical Treatment of Solvation for Molecular Mechanics and Dynamics. **Journal of the American Chemical Society,** v. 112, n. 16, p. 6127-6129, 1990.

THOMAZELLA, D. P. T.; TEIXEIRA, P. J. P. L.; OLIVEIRA, H. C.; SAVIANI, E. E.; RINCONES, J.; TONI, I. M.; REIS, O.; GARCIA, O.; MEINHARDT, L. W.; SALGADO, I.; PEREIRA, G. A. G. The hemibiotrophic cacao pathogen Moniliophthora perniciosa depends on a mitochondrial alternative oxidase for biotrophic development. **New Phytologist,** v. 194, n. 4, p. 1025-1034, 2012.

WOO, E. J.; MARSHALL, J.; BAULY, J.; CHEN, J. G.; VENIS, M.; NAPIER, R. M.; PICKERSGILL, R. W. Crystal structure of auxin-binding protein 1 in complex with auxin. **Embo Journal,** v. 21, n. 12, p. 2877-85, 2002.

ZAPAROLI, G.; CABRERA, O. G.; MEDRANO, F. J.; TIBURCIO, R.; LACERDA, G.; PEREIRA, G. G. Identification of a second family of genes in Moniliophthora perniciosa, the causal agent of witches' broom disease in cacao, encoding necrosis-inducing proteins similar to cerato-platanins. **Mycological Research,** v. 113, p. 61-72, 2009.